Experiment:
Doppler-free saturation spectroscopy of Rubidium

Physical Internship PPBphys2

in Summer Semester 2021

Executed on 13.09.2021 from

Konstantin Rausch und Lydia Ploss

Supervisor: Jana Sanchayeeta

Inhaltsverzeichnis

1 Motivation and Purpose of the Experiment

With doppler-free saturation spectroscopy the molecular structure of elements can get analysed.
In this experiment a gas cell containing the isotopes ^{85}Rb and ^{87}Rb gets exposed to 3 laser beams of different intensities coming from the same laser source. The recorded spectrum contains absorption and hyperfine peaks. Out of the positions and distances of the seperate peaks transition energies can be calculated. This not only gives insight on the structure of the elements but also the ratio of the rubidium isotopes can be calculated.

2 Questions for preparation

2.1 Nuclear spins and quantum numbers of the two rubidium isotopes

The nuclear spin of an atom depends on the structure of the nucleus. Rubidium has an atomic number of 37. Therefore the nucleus of ^{85}Rb consist of 37 protons and 48 neutrons, whereas ^{87}Rb has 37 protons and 50 neutrons. Both isotopes have an even number of neutrons and an uneven number of protons, which leads to a nuclear spin that is a multiple of $\frac{1}{2}$. The factor that is multiplied with $\frac{1}{2}$ depends on the total spin of the nucleons the nucleus consists of.
Because ^{85}Rb and ^{87}Rb only differ in 2 neutrons, they have different nuclear spins that are both multiples of $\frac{1}{2}$.

	$5^2S_{\frac{1}{2}}$	$5^2P_{\frac{1}{2}}$	$5^2P_{\frac{3}{2}}$
S	$\frac{1}{2}$	$\frac{1}{2}$	$\frac{1}{2}$
L	0	1	1
J	$\frac{1}{2}$	$\frac{1}{2}$	$\frac{3}{2}$
I	$\frac{5}{2}$	$\frac{5}{2}$	$\frac{5}{2}$
F	2, 3	2, 3	1, 2, 3, 4

Tabelle 2.1: quantum numbers of ^{85}Rb

	$5^2S_{\frac{1}{2}}$	$5^2P_{\frac{1}{2}}$	$5^2P_{\frac{3}{2}}$
S	$\frac{1}{2}$	$\frac{1}{2}$	$\frac{1}{2}$
L	0	1	1
J	$\frac{1}{2}$	$\frac{1}{2}$	$\frac{3}{2}$
I	$\frac{3}{2}$	$\frac{3}{2}$	$\frac{3}{2}$
F	1, 2	1, 2	0, 1, 2, 3

Tabelle 2.2: quantum numbers of ^{87}Rb

2.2 Types of Broadening

Transitions in atomic spectra are always not completely sharp. Instead the form of the lines differs from the ideal form of a delta-function peak by having a finite width.

Natural broadening

The most basic form of broadening happening in atomic spectra is the natural line width. Th cause of this effect lies in the very nature of atoms. The Uncertainty relation of quanten physics links the finite lifetime of an excited state (radiative decay) with the uncertaincy of its energy.

$\Delta E = \frac{h}{2\pi\tau_i}$

This means that a short lifetime results in a large energy uncertainty and a broad emission resulting in a Lorentzian profile. This natural broadening is only infuencable

very slightly by artificially suppressing or enhancing decay rates of the involved atoms. The transition of an atom from state i to another state j results in: $\Delta\nu = \frac{\delta E}{h} = \frac{1}{2\pi\tau}$

Doppler broadening

This broadening effect is due to the Doppler effect caused by a distribion of velocities of atoms or molecules. The line is broadened because of Doppler shifts that are caused by emitting particles with different velocities. Due to the thermal movement of the atoms in a gas, each atoms is moving at a different speed in different directions. From the observer, each atom is red or blue shifted by the Doppler effect depending of its velocity. The higher the temperature, the bigger the doppler shift and therefore a broader line. The form of the broadening effect is described by a Gaussian profile. The linewidth resulting from the Doppler effect is:
$\Delta\nu_D = \frac{2\nu_0}{c}\sqrt{2\ln 2\frac{k_B T}{m}}$ with ν_0 being the mean of optical frequency and m the mass of the atoms. This broadening is typically much larger than the natural linewidth.

Homogeneous/inhomogeneous and saturation widening

Widening is a process through which the line width is increased more than the natural line width would have been.

Homogenous widening occurs when the propability of emission at a certain frequency is the same for all particles (saturation broadening).

Inhomogenous widenig is the exact opposite. It occurs when the emission uncertainty is not the same for all particles (Doppler broadening)

Lasers with high intensities can cause saturation. The parameter describing this saturation is defined as: $S(\omega) = S(\omega_0)\frac{(\frac{\gamma}{2})^2}{(\omega-\omega_0)^2+(\frac{\gamma}{2})^2}$ In this manner ω_0 is the frequency of resonance of the transition that is being observed and γ is the natural line width. The absorption rate of this transition is defined as: $\alpha(S) = \alpha_0(\omega_0)\frac{(\frac{\gamma}{2})^2}{(\omega-\omega_0)^2+(\frac{\gamma_S}{2})^2}$ with $\alpha_0(\omega_0)$ being absorption rate of the unsaturated state. This describes a Lorentzian profile with the half-life width of $_S = \gamma\sqrt{1+S(\omega_0}$. The saturation of this transition prevents a occupation over $\frac{1}{2}$. Therefore, hight pump rates lead to more photons being absorbed at the borders of the spectral line, increasing the width.

2.3 Cross-over resonances

If there are two (or more) excited states that can have transitions with the same ground state and the difference between the transition frequencies is smaller than the Doppler-width, cross-over resonances arise. Cross-over resonances are local minima that appear in the absorption profile that are no lamp dips.
If for example the pump beam can excite the transition from ground to first excited state and the sample beam excites the transition from ground to second excited state, then much more atoms get excited to the first excited state because the intensity of the pump beam is much higher than of the sample beam. Because both beams excite atoms from the same ground state, the sample beam has not much atoms

on the ground state left that it can excite to the second excited state. Therefore the absorption curve has a local minimum at the laser frequence where pump beam excites to first and sample beam to second excited state.

2.4 Beam splitter cubes, $\lambda/2$ plate and filter wheel

The first beam splitter cube is used to split the laser beam into three seperate beams. Firstly the incoming beam is splitted into the pump beam and another beam by using a polarising beam splitter. Then the other beam is splitted again into sample and reference beam using a 50:50 beam splitter.
Through a polarising splitter only waves of certain polaristions transmit, the other ones get reflected. This is used to create two beams with different intensities, which is essential because the pump beam needs to have a much bigger intensity than the sample beam.

The $\frac{\lambda}{2}$ plate is used to regulate the intensity of the incoming laser beam, whereas the filter wheel can be used to adjust the intensities of the splitted beams.

2.5 Hyperfine structure

By measuring the absortion spetra of the rubidium isotopes , the position of the absorption lines is know. With this information, the energy of absorption for this particular transition can be calculated:

$$\Delta E_{HFS} = \frac{a}{2}[F(F+1) - J(J+1) - I(I+1)]$$

For the rubidium isotopes we are dealing with F, J and I are known, making it possible to calculate a from the given equation

$$a = \frac{g_I \mu_K}{\sqrt{J(J+1)}}$$

with g_I being the Lande-factor of the atomic core and $\mu_K = \frac{eh}{2m_P} = 5.0510 \cdot 10^{-27}$ being the magneton of the core. For the possible transitions the selection rules of the hyperfine struture have to be used: $\Delta L = \pm 1$, $\Delta J = 0, \pm 1$ and $\Delta F = 0, \pm 1$. ALso the D_1 and D_2 lines have to be looked at seperately.

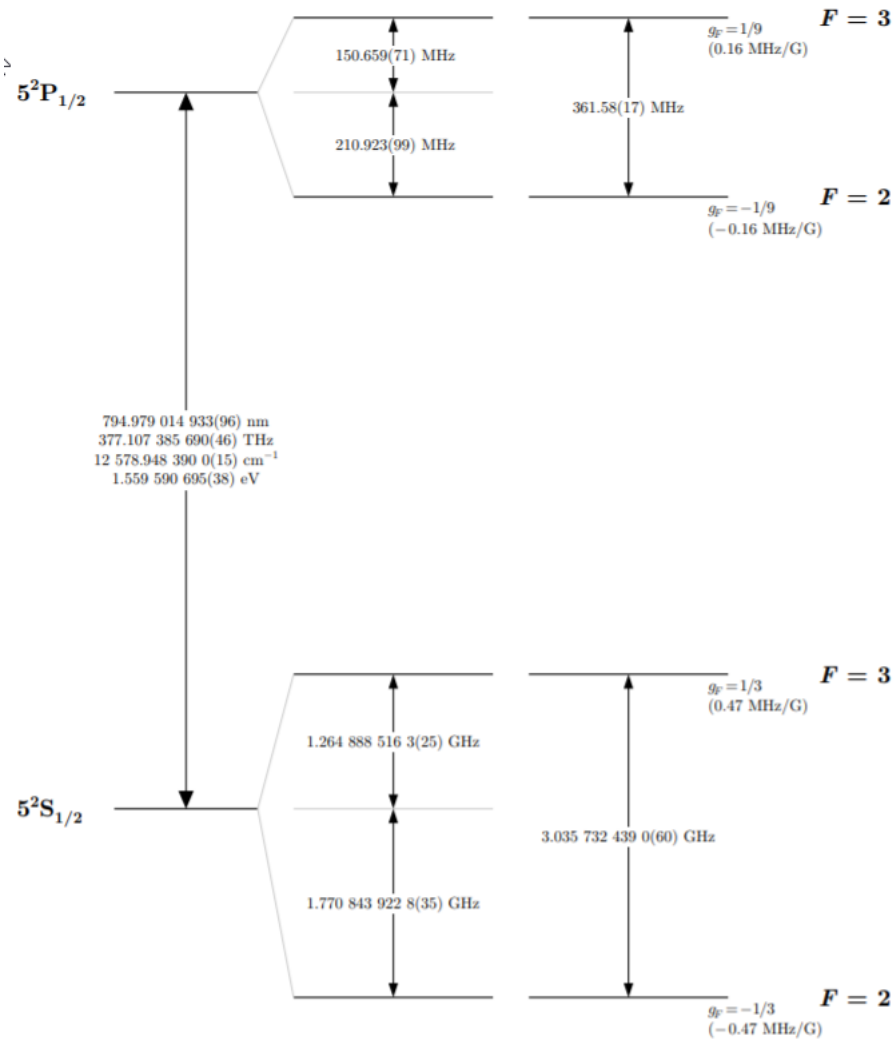

Abbildung 2.1: Possible Transition of the D_1-line for Rb^{85},
Quelle : *https* : *//steck.us/alkalidata/rubidium*85*numbers.pdf*

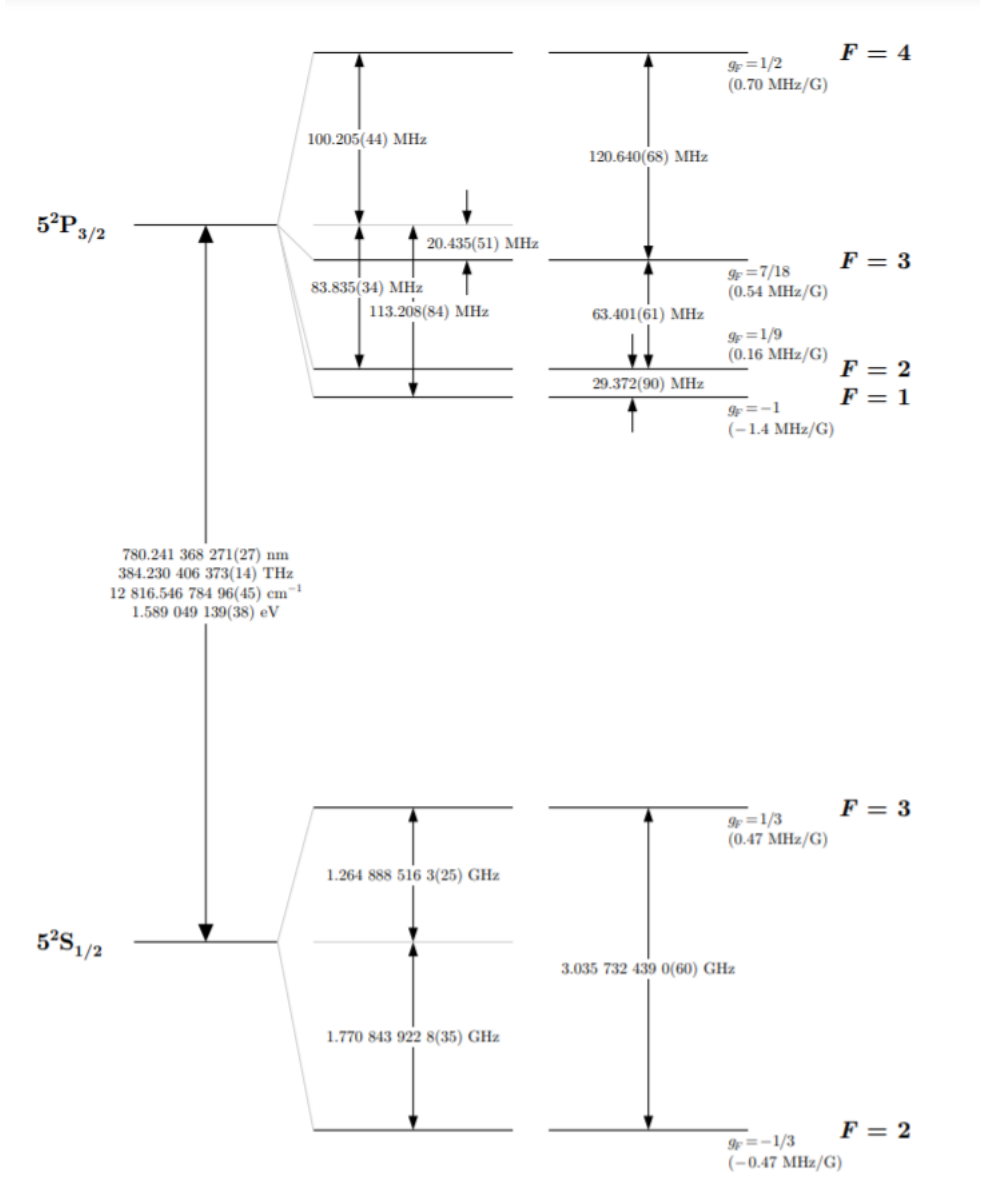

Abbildung 2.2: Possible Transition of the D_2-line for Rb^{85},
Quelle : *https* : *//steck.us/alkalidata/rubidium*85*numbers.pdf*

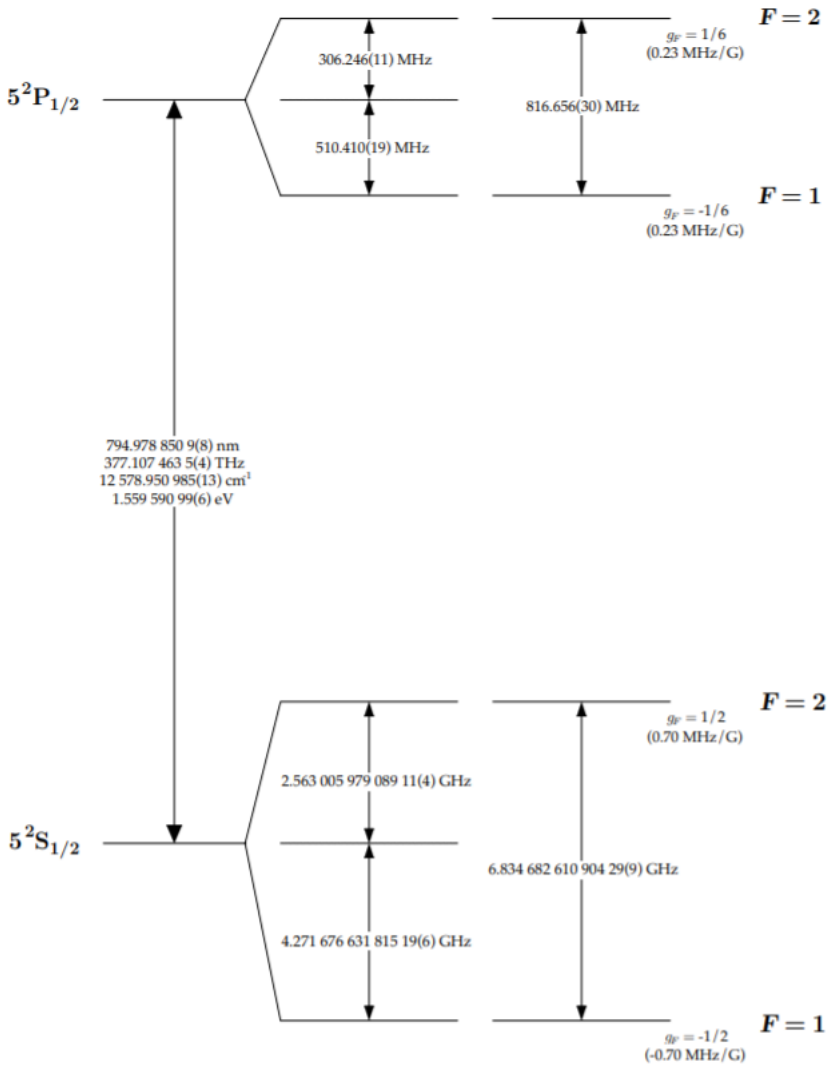

Abbildung 2.3: Possible Transition of the D_1-line for Rb^{87},
Quelle : *https* : *//steck.us/alkalidata/rubidium*87*numbers*.1.6.*pdf*

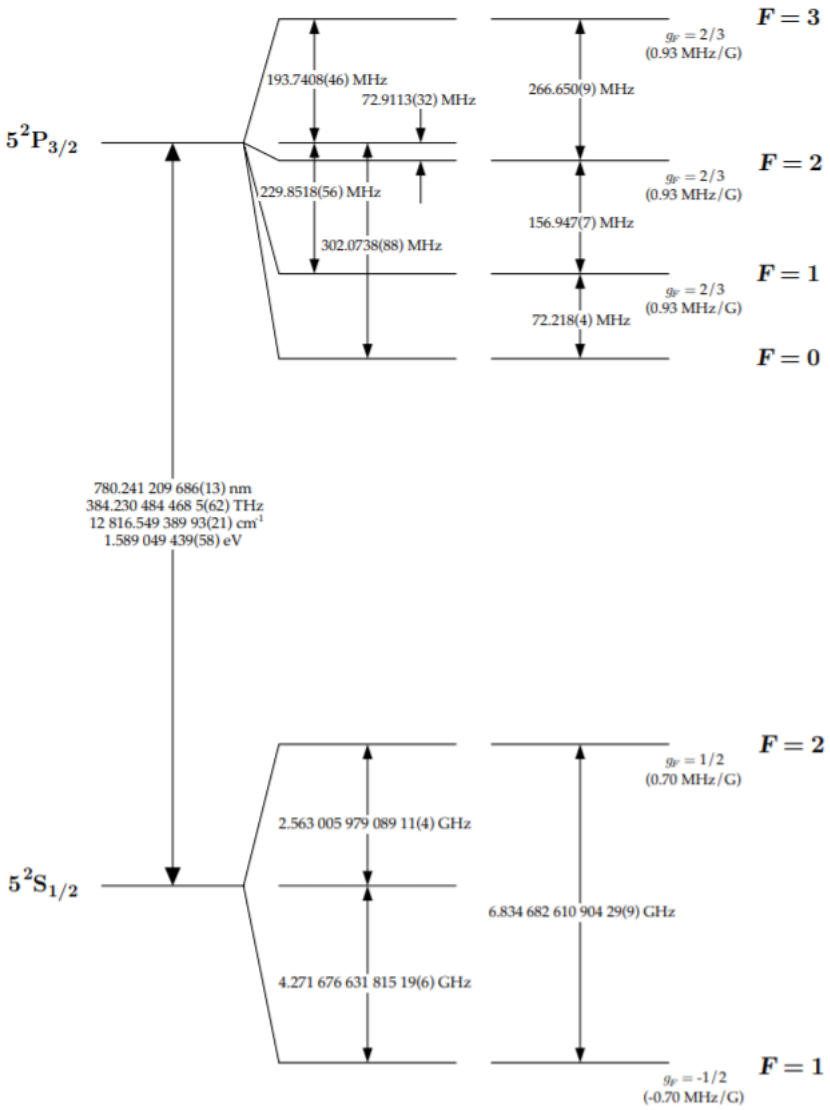

Abbildung 2.4: Possible Transition of the D_2-line for Rb^{87},
Quelle : *https* : *//steck.us/alkalidata/rubidium87numbers*.1.6.*pdf*

3 Experimental Procedure

Measurements were taken at temperatures of the gas cell of 23 °C, 40 °C and 60 °C. For every temperature the absorption spectrum of all 4 lines were measured as well as the spectrum of every line seperately. The channels that were activated in the program while taking the measurements were: 0, 1, 3 and 4.
This means:

channel	meaning
0	overlap of sample and reference beam
1	sample beam
3	reference beam
4	Fabry-Pérot interferometer

4 Evaluation

It was chosen to use a gas temperature of 40 ° C to carry out the evaluation with because it seemed to be a good compromise between the height of the lamp dips and the width of the lines.
The linewidth resulting from the Doppler effect is proportional to the temperature (2.2). Therefore with rising temperatures the linewidth gets bigger. However the peaks coming from lamp dips get stronger with higher temperatures.

4.1 Freeing the Absorption Spectrum from Trends

To free the absorption spectrum from trends a linear regression was fitted through the functions of sample and reference beam and the function of the Fabry-Pérot interferometer. Then the values of the fitted function were subtracted from the values of the measured function. This created functions of the absorption spectrum that are free from trends.

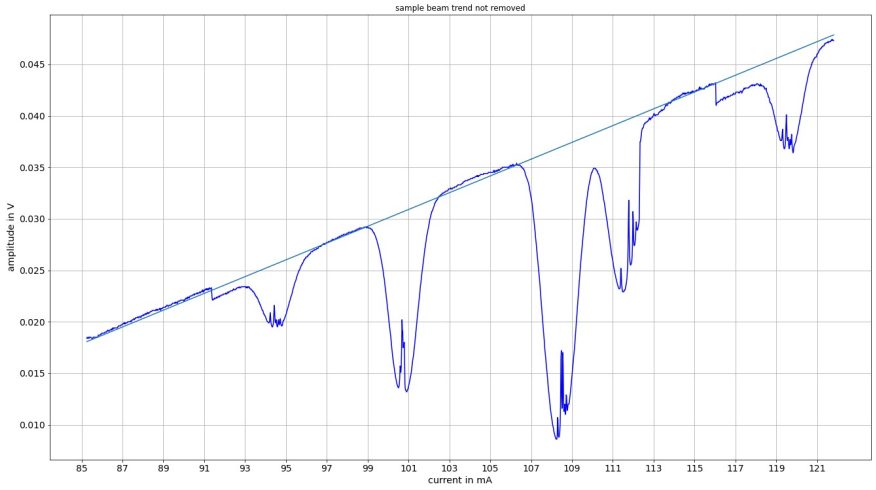

Abbildung 4.1: sample beam with trend and fitted line

Now that the measured data is free from trends, the lines can be identified. However the quality of the data is not quite high enough to identify the lines unprobematically,

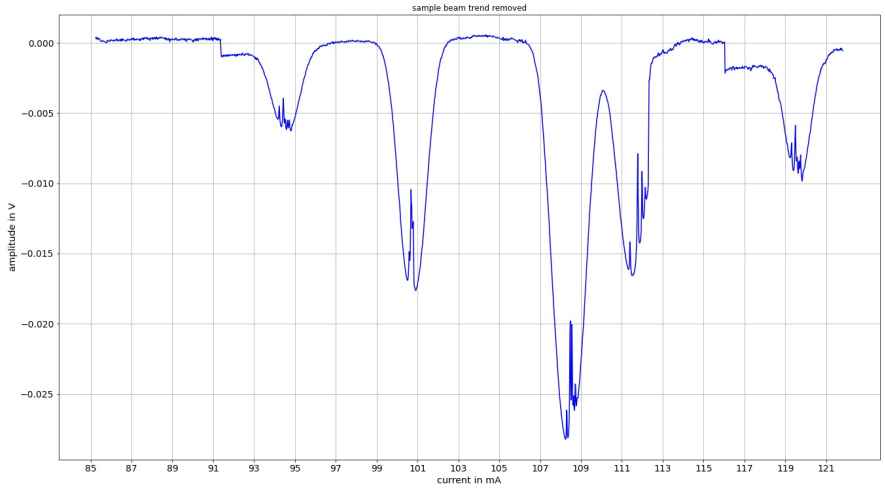

Abbildung 4.2: sample beam trend removed

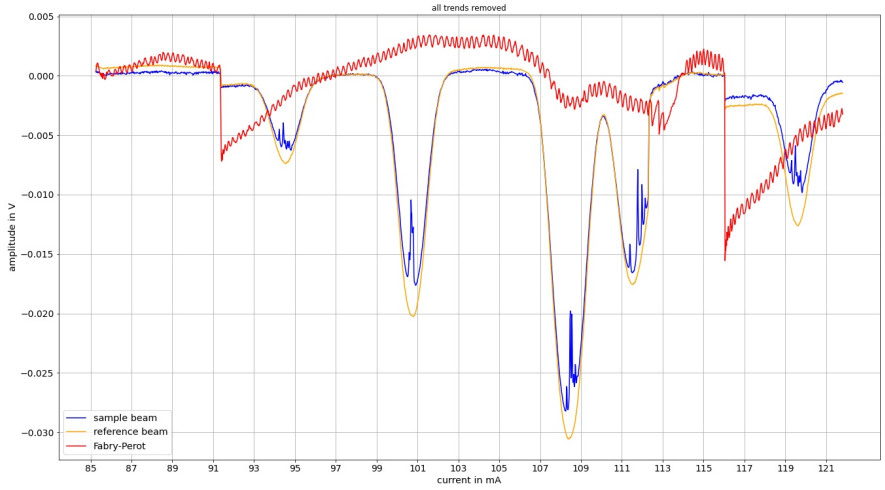

Abbildung 4.3: all channels trend removed

because the distances between the different minima are extremely small. Not being able to differentiate between the different transitions clearly, leads us to try two seperate ways of assigning the data. The position of the peaks in laser current is transformed into wavelength in order to be able to compare them to the values found in the literature.

Only considering the order
By looking at the data, it seems to be very apparant in which order the peaks appear. Therefore one can try to assign the different lines by order, comparing them to the order of the data from the literature.

Peak (current)	measured wavelength in nm	wavelength from literature in nm	rubidium isotope	F	deviation in nm
1	780.239	780.244	^{85}Rb	3	$5{\cdot}10^{-3}$
2	780.245	780.246	^{87}Rb	2	$1{\cdot}10^{-3}$
3	780.2325	780.233	^{87}Rb	1	$5{\cdot}10^{-4}$
4	780.2355	780.238	^{85}Rb	2	$2.5{\cdot}10^{-3}$

Tabelle 4.1: Identification by order

The accumulated deviation for this method is $9 \cdot 10^{-3}$. But looking more into the resulting assignment of peaks, it becomes apparant that, opposing the expectation, the peaks with the highest intensity are the ones assigned to ^{87}Rb. This is contradicting, because ^{85}Rb is the isotope that is supposed to be in a higher concentration and therefore have larger peaks.

Considering intensity and order
In order to circumvent the problem of unfitting intensities of isotopes, the peaks are foremost assigned by intensity, meaning the peaks of higher intensity are the ones of ^{85}Rb. Then the two peaks are seperately identified by considering the order.

Peak (current)	measured wavelength in nm	wavelength from literature in nm	rubidium isotope	F	deviation in nm
1	780.2390	780.233	^{87}Rb	1	$6{\cdot}10^{-3}$
2	780.2450	780.238	^{85}Rb	2	$7{\cdot}10^{-3}$
3	780.2325	780.244	^{85}Rb	3	$11.5{\cdot}10^{-3}$
4	780.2355	780.246	^{87}Rb	2	$10.5{\cdot}10^{-3}$

Tabelle 4.2: Identification by intensity and order

The accumulated deviation for this method is $9 \cdot 10^{-3}$. It becomes visible that this method has a lot larger deviation.

4.2 Distances between Energy Levels

4.2.1 Using the Enclosed Current Wavelength Characteristic Curve

In order to transform the axis of the recorded data from laser current to frequency, the given transformation sheet has to be used.

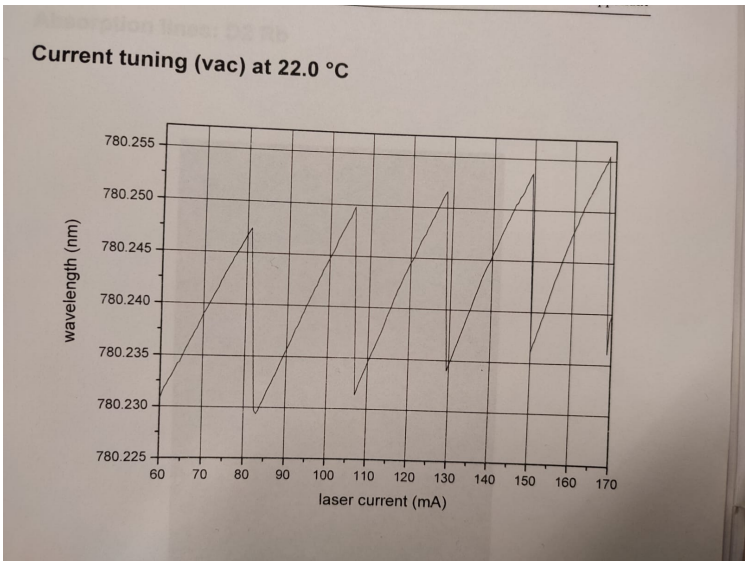

Abbildung 4.4: Transformation sheet for the experiment

Thus the recorded data is transformed into wavelenght first. The order of the peaks is changed, because two of the four peaks are located on another current/wavelength slope than the other two. In the next step, wavelength is transformed to frequency by using the formular $\nu = \frac{c}{\lambda}$. Now having transformed the x-axis to the desired format, the distance between the peaks can be determined.

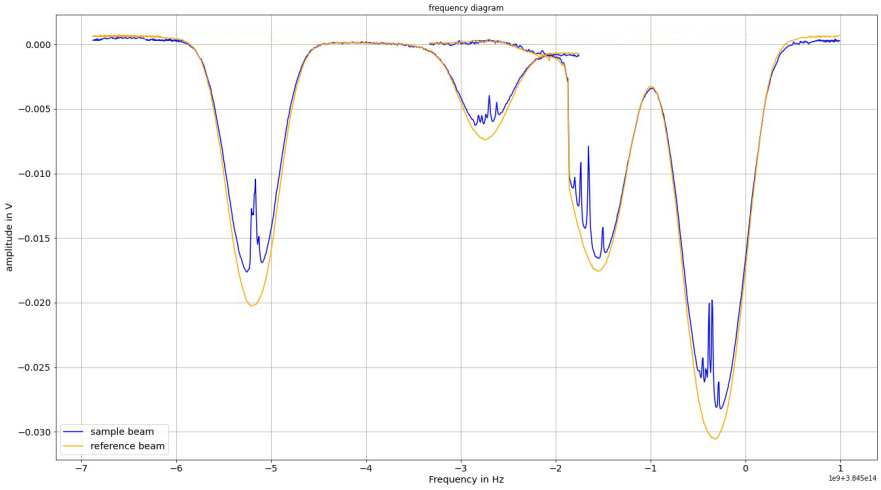

Abbildung 4.5: Measured data transformed to frequency axis

By looking at the diagram you can see some uncharacteristic data between peak two and three (counting from the left). These unfitting data points occur because of the not optimal transformation from current to wavelength. The exact location of the jump in wavelength is hard to translate onto the data and therefore a section of overlapping occurs. However these data points do not have a meaning behind them and can neglected.

peak transition	distance between the peaks in 10^8Hz
$1 \rightarrow 2$	24.50
$2 \rightarrow 3$	11.50
$3 \rightarrow 4$	13.00

Tabelle 4.3: distances between the energy levels of the absorption spectrum (peaks counted from left to right)

4.2.2 Using the Fabry-Pérot interferometer

To calculate the relative frequences between the energy levels the function of the Fabry-Pérot interferometer is used.
The distance between two peaks of the function can be calculated by using the equation:

$$\Delta\omega_{FSR} = \frac{c}{2nd} = \frac{c}{2d} \qquad \text{(n=1 because it was measured in air)}$$

The distance d can be calculated out of the seperate distances between the mirrors of the interferometer:

$$d = 81\,\text{cm} + 35\,\text{cm} + 42\,\text{cm} - 9\,\text{cm} = 1,49\,\text{m}$$

$$\Delta\omega_{FSR} = \frac{3 \cdot 10^8 \text{m}}{2 \cdot 1,49 \text{m s}} = 1,0067 \cdot 10^8 \text{ Hz}$$

The trendfree function of the Fabry-Pérot interferometer has no linear course. Only in small intervalls it is an approximate straight line. Therefore only the part between 101 and 105 mA was used to count the peaks. In this intervall of 4 mA, 15 distances between two peaks were counted.

$$15\,\Delta\omega_{FSR} \cdot \frac{1\,\text{mA}}{4\,\text{mA}} = 3,7751 \cdot 10^8 \text{ Hz}$$

This means that the distance of 1 mA corresponds to $3,7751 \cdot 10^8$ Hz. Now the distances between the minima of the beam function can be converted from current to frequence. As it was seen in 4.2.1 the order of the peaks gets changed by tranforming current to wavelength, because all 4 peaks don't lay on the same slope of the characteristic curve. That leads to the minimum that is at the highest current having the smallest wavelength. Therefore only the two distances between the three peaks that didn't change their order by getting tranformed to wavelength can be compared to 4.2.1.

number of peak	current in mA
1	94,562
2	100,807
3	108,403
4	111,542

Tabelle 4.4: current of the peaks

difference between peaks	difference of current in mA	difference of frequence in 10^8 Hz
2-1	6,25	23,58
3-2	7,60	28,72
4-3	3,14	11,86

Tabelle 4.5: differences of current and frequences between peaks

4.3 Ratio of the two rubidium isotopes

In the following the true ratio of the two isotopes should be calculated. Therefore the area underneath the peaks has to be determined. To do this we chose the trend free data so that the fit is more accurate. The choice of the x-axis (current, wavelength, frequency) is completly irrelevant because it does not have an influence on the relation of area under the peaks.

The function that is being fitted onto the data has the form $y - ae^{-\frac{(x-x_0)^2}{2c^2}}$

Peak	a	x_0	c	y
1	7.04024110e-03	9.45189373e+01	6.30491494e-01	-3.72985846e-04
2	2.15210937e-02	1.00752432e+02	6.55067601e-01	7.83556418e-04
3	3.29933593e-02	1.08430576e+02	7.83077181e-01	1.63135265e-03
4	1.79329322e-02	1.11480158e+02	6.43772505e-01	-2.04670166e-04

Tabelle 4.6: Fitting data for the different Peaks

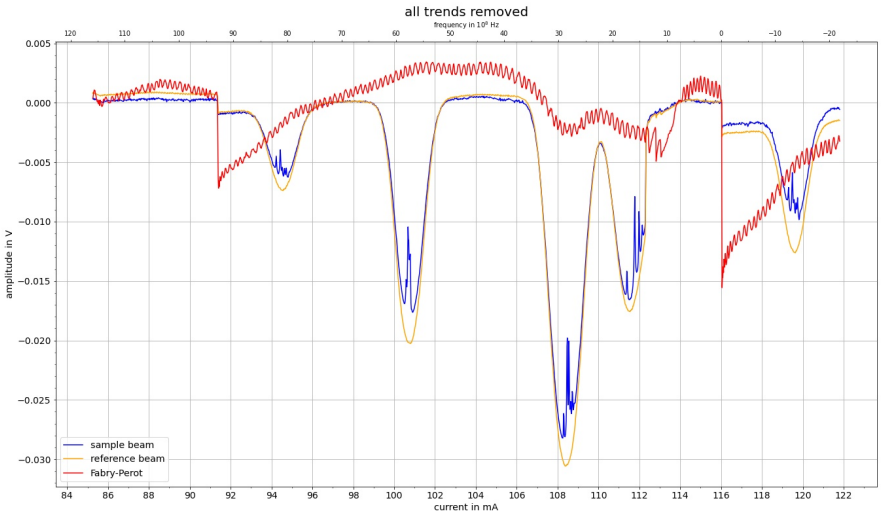

Abbildung 4.6: trendfree spectrum with current and frequences

With this knowledge of the parameters of the fitted gaussians, we can calculate the area.

With the relation: $\int_{-\infty}^{\infty} e^{-a(x+b)^2}\,dx = \sqrt{\frac{\pi}{a}}$

we can solve our equation: $\int_{-\infty}^{\infty} ae^{-\frac{(x-x_0)^2}{2c^2}}\,dx$

by identifying $b = x_0$ and a=$\frac{1}{2c^2}$ and neglecting y, because we only want to look at

the area under the peak.
We can calculate the area as: $\int_{-\infty}^{\infty} ae^{-\frac{(x-x_0)^2}{2c^2}}\,dx = -a\sqrt{2\pi c^2}$

Peak (current)	rubidium isotope	area
1	^{85}Rb	-0.016680
2	^{87}Rb	-0.035338
3	^{87}Rb	-0.064762
4	^{85}Rb	-0.028938

Tabelle 4.7: areas under the current peaks with peak assignment 1 from 4.1

Peak (current)	rubidium isotope	area
1	^{87}Rb	-0.016680
2	^{85}Rb	-0.035338
3	^{85}Rb	-0.064762
4	^{87}Rb	-0.028938

Tabelle 4.8: areas under the current peaks with peak assignment 2 from 4.1

The area under the peaks is proportional to the amount of atoms of the corresponding isotope in the gas cell. Therefore one can sum up the areas under the peaks of one particular isotope and devide it by the area of both isotopes in order to get the percentage of isotope in the cell. This results in:

Assignment considering order from 4.1

^{87}Rb: $\frac{0.035338+0.064762}{0.035338+0.064762+0.016680+0.028938} = 0.687$

Meaning there would be 68.7% of ^{87}Rb and 31.3% of ^{85}Rb being the complete opposite of what was to be expected.

Assignment considering intensity and order from 4.1

Because this assignment of lines is exactly opposite from the other methode, there would be 31.3% of ^{87}Rb and 68.7% of ^{85}Rb. This relation of concentration is very close to the one given in the instruction, which is 72.2% for ^{85}Rb and 27.8% for ^{87}Rb.

4.4 Hyperfine Dips

The plots of the absorption dips are listed below. The numbers of the peaks refer to the current axis, this means that peak number 1 has the lowest current and peak number 4 the highest.

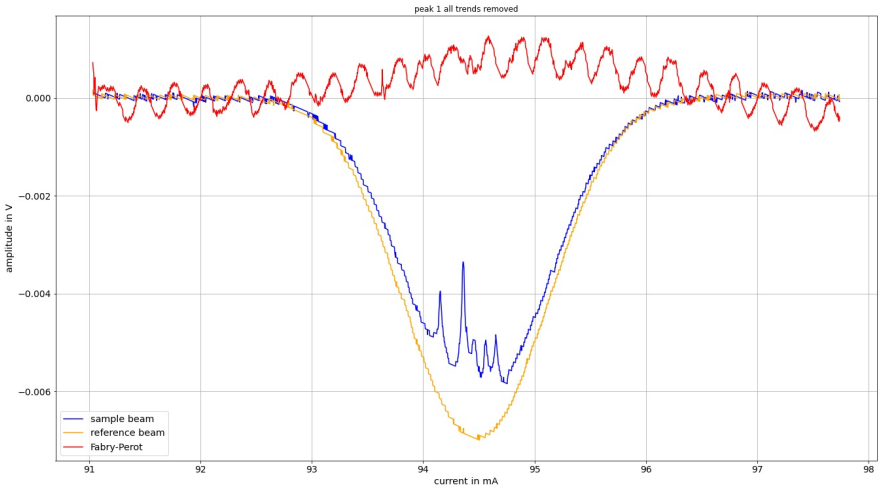

Abbildung 4.7: absorption spectrum of peak number 1

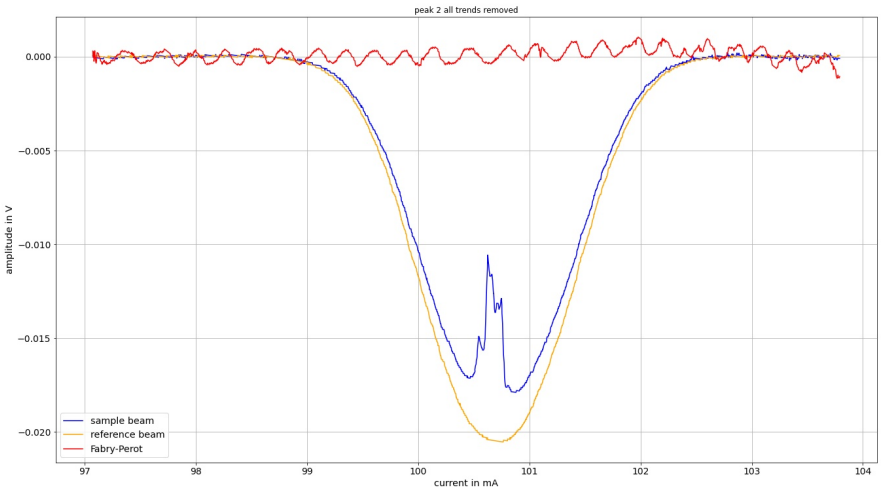

Abbildung 4.8: absorption spectrum of peak number 2

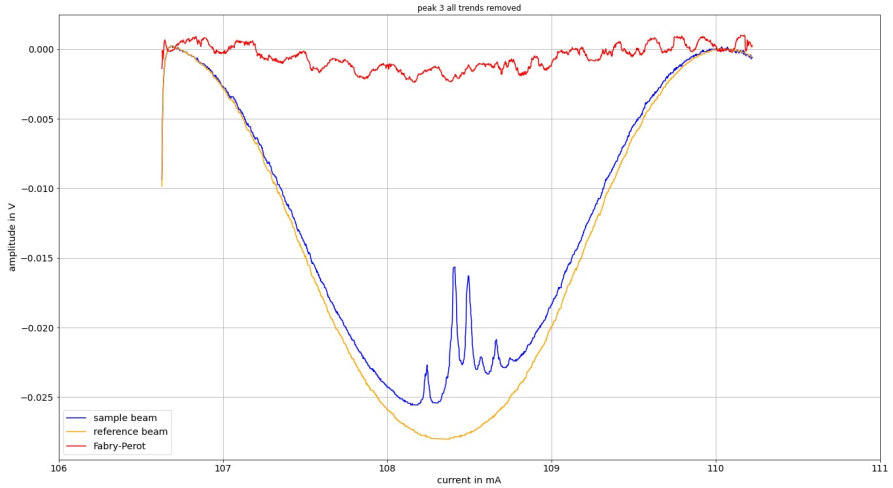

Abbildung 4.9: absorption spectrum of peak number 3

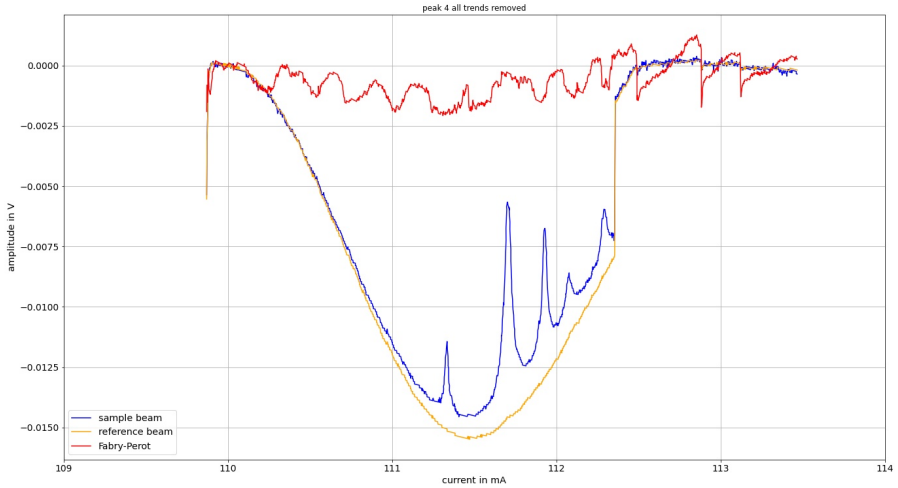

Abbildung 4.10: absorption spectrum of peak number 4

Peak number 3 was chosen to fit the lorentz curves at. The fit was created with the lorentz function:

$$l(x) = y - \frac{a \cdot w^2}{(x-c)^2 + w^2}$$

Furthermore bounds were set to achive the optimal fit.

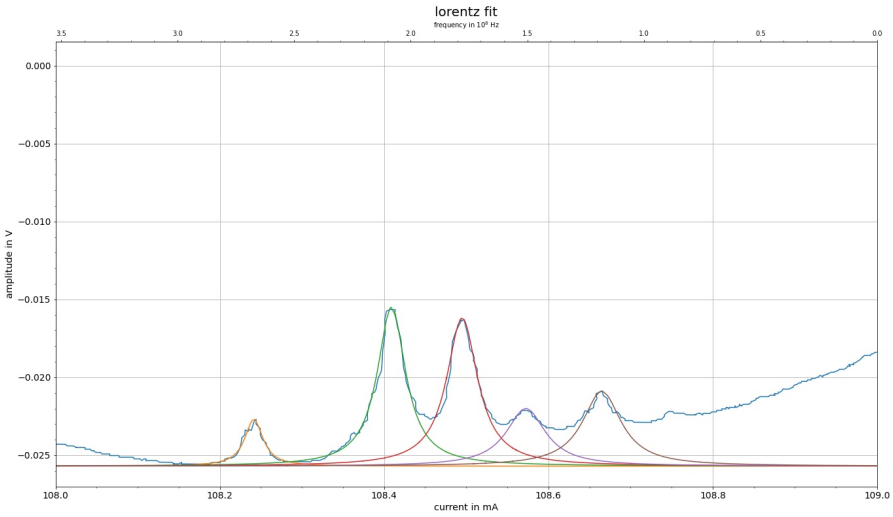

Abbildung 4.11: absorption spectrum of peak number 3 with lorentz curves

The current of the maximum of each hyperfine dip is described by parameter c. The current values can be transformed into wavelength by using the linear regression that was fitted through the line of diagram 4.4 at current values of 108 mA to 127 mA.

number of hyperfine dip	position in mA	position in nm
1	108,24146	780,232849
2	108,40900	780,233009
3	108,49500	780,233090
4	108,57260	780,233164
5	108,66737	780,233255

Tabelle 4.9: positions and distances of dips at peak 3

The first thing you notice is that there are more peaks than hyperfine transitions are possible. Each absorption peak resembles all transitions that are possible starting from the same energy level at a specific F. This means that in each peak should be found three hyperfine dips, because the selection rule for hyperfine transitions is $\Delta F = 0, \pm 1$ and therefore there are 3 possible hyperfine transisitions. The other dips therefore could only come from cross over references (2.3).
To assign three of the 5 peaks to hyperfine transitions the positions of the peaks in nm can be compared to literature values. In 4 two methods were presented on how to match the absorption peaks to possible transitions. Depending on the method, peak number 3 can either be starting from ground state F=1 of ^{87}Rb or F=3 of ^{85}Rb. Only method 1 ("Only considering the order") fits the wavelength of the measured absorption dips, method 2 gives a wavelength that is too big. Therefore method 1 is

chosen to match hyperfine dips to possible hyperfine transitions.

number of hyperfine dips	measured position in nm	measured distance in MHz	transition literature (F values)	position from literature in Hz	distance from literature in MHz
1	780,232849		$1 \rightarrow 2$	780,232684	
2	780,233009	78,5771	$1 \rightarrow 1$	780,233002	72,2220
4	780,233164	76,7311	$1 \rightarrow 0$	780,233149	156,9406

Tabelle 4.10: positions and distances of hyperfine dips at peak 3

After comparing with literature peaks number 1, 2 and 4 seem to be coming from hyperfine transitions. As a consequence it can be said that peak number 3 and 5 have to be coming from cross over resonances.
The magnitude of measured positions and distances fits the literature ones. But especially for hyperfine dip number 4 there are discrepancies that can't be unseen.

4.5 Hyperfine Structure Constants

The hyperfine structure contant can be calculated using the equation from 2.5:

$\Delta E_{HFS} = \frac{a}{2}[F(F+1) - J(J+1) - I(I+1)]$

The constant a can then be calculated when knowing the quantum numbers and energies of two transitions from ground state to two seperate excited states as following:

$a = \frac{2(\Delta E_2 - \Delta E_1)}{F_2(F_2+1) - F_1(F_1+1)}$

(J and I have always the same values and therefore cancel themselves)

To calculate the hyperfine structure constant the distances between the hyperfine dips of ^{87}Rb from table 4.10 were taken.

distance between F states	a_{measured} in 10^{-26} J	$a_{\text{literature}}$ in 10^{-26} J
$0 \rightarrow 1$	5,0843	4,7855
$1 \rightarrow 2$	5,2066	5,1995

Tabelle 4.11: hyperfine structure constants

4.6 Calculating Gas Temperatures

In order to calculate the temperature of the gas, the formular from the questions for preparation can be utilized:

$$\Delta\nu_d = \frac{2\nu_0}{c}\sqrt{2ln(2)\frac{k_B T}{m}}$$

In this formular $\Delta\nu_d$ is the peak width at half-height, ν_o is the frequency of the peak at its highest intensity and T is the temperature.
At first the peak width at half-height has to be calculated. This can be done by fitting a function $g(x) = \frac{1}{\sqrt{2\pi\sigma^2}exp(-\frac{(x-x_0)^2}{2\sigma^2}}$ to the data. The fitted value for σ can be used to calculate the desired width:

$$\Delta\nu_d = 2\sqrt{2ln(2)}\sigma$$

Now the temperature can be calculated using the formular above and the velocities can be determined.

Most probable velocity: $\hat{v} = \sqrt{\frac{8k_B T}{\pi m}}$
Mean velocity: $\bar{v} = \sqrt{\frac{8k_B T}{\pi m}}$

It is most favorable to chose a peak that is very clear and has an almost perfect shape. Therefore we chose peak 2 from the current spectrum, which we decided to assign to ^{87}Rb (F=2) after the results of 4.4. For the fit, we also calibrated the frequency using the Fabry-Perot interferometer.

$\Delta\nu_D in 10^8$Hz	T_{Theo} in K	T in K	$\hat{v}$	$\bar{v}$
4.610	296.45	243.92	216.03	229.41
5.0859	311.06	296.88	238.34	268.93
6.3497	329.25	462.75	297.56	335.76

Tabelle 4.12: Calculated gas temperatures and velocities

It is apparant, that the calculated values for the gas temperatures differ quite a lot from the actual values that were adjusted during the experiment. But you can see that the scale is right and that the line width increases with higher temperatures. This method of calculating the gas temperature is not optimal because the assignment of the peaks and the transformation from current to wavelength is not accurate enough to be able to recognize such slight differences that are occuring during this experiment.

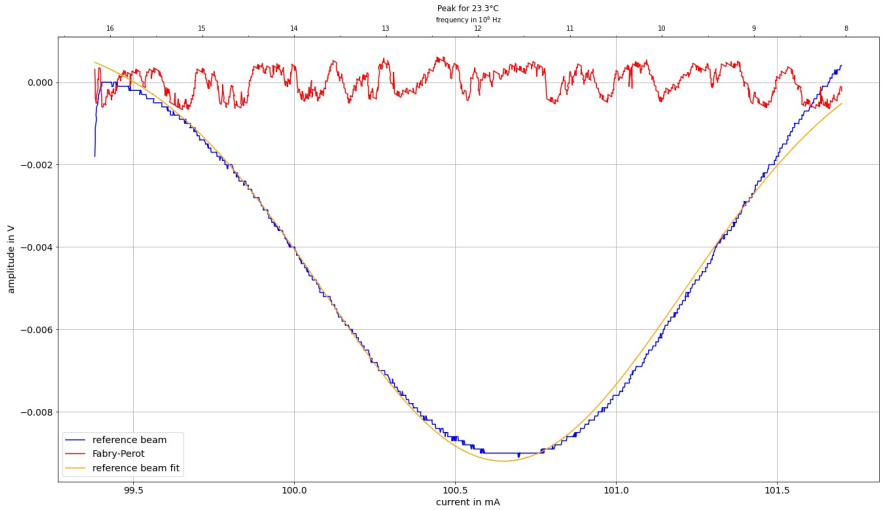

Abbildung 4.12: Peak 2 (current) for 23.3°C

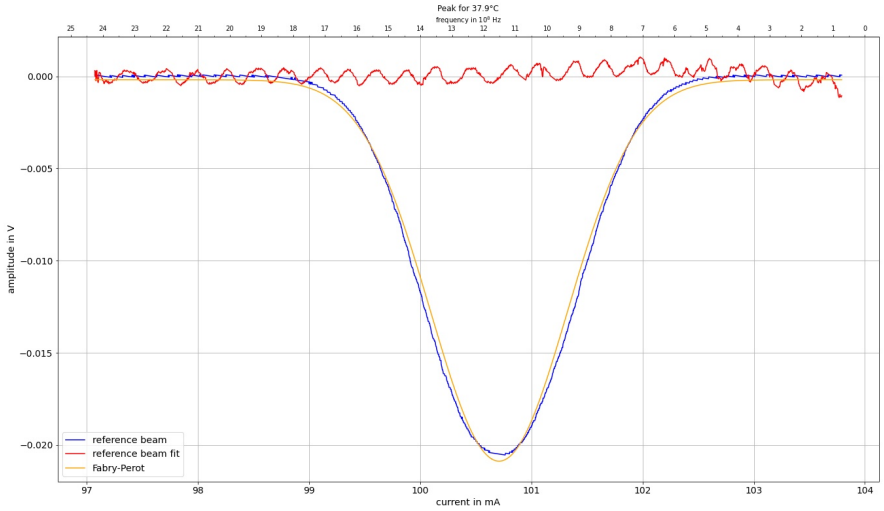

Abbildung 4.13: Peak 2 (current) for 37.9°C

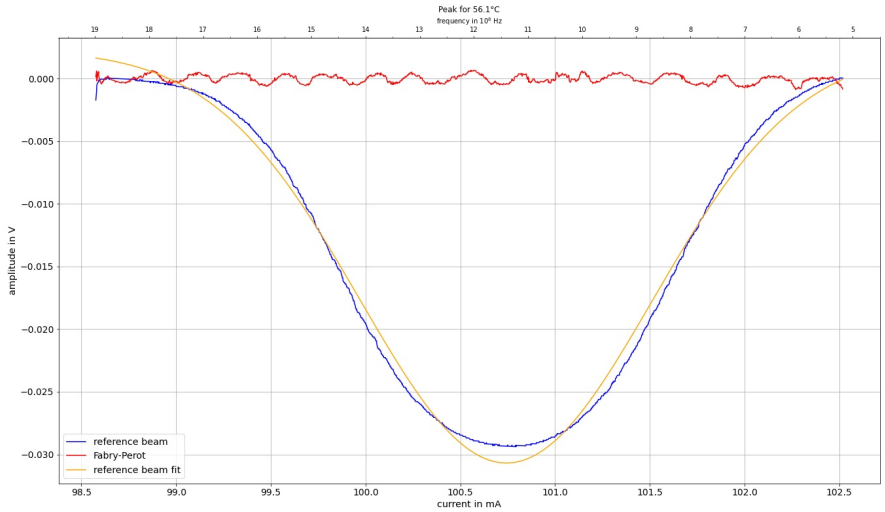

Abbildung 4.14: Peak 2 (current) for 56.1°C

5 Summary and Conclusion

During this experiment and the later evaluation of the measured data, it becomes apparent how small the regarded transitions within the atoms are and how precise the measurements have to be in order to be able to identify the hyperfine structures. At the same time it is extremely impressive that we were able to detect such small signals with a rather uncomplex composition of tools. It was also interessting to experience the learned theory of hyperfine structure in the true world.